1   Ammonia Synthesis and Storage

1.1   Introduction

1.1.1   Overview

This section encompasses the processes required to produce and store the quantities of ammonia needed to meet the electricity demand of Maui. This includes both the ammonia synthesis stage and the long-term storage methods required in meeting demand, as well as a brief design of an ammonia cracker. However, it is first wise to consider the overall need for the production and storage of ammonia. Hydrogen is produced from wind energy in electrolysis. In theory, this can be stored directly and used to fuel a gas turbine or fuel cell, thus the need for ammonia is not immediately clear. However, a comparison of the properties of the hydrogen and ammonia in Table **??** shows significantly higher energy density of ammonia, as well as the pressure and temperature requirements being significantly closer to atmospheric conditions. This in turn means the cost of storage infrastructure and power requirements are hugely more economical in the case of ammonia.

Table 1: Hydrogen and Ammonia energy storage properties and the conditions required [4]

Substance	Liq. energy density	Boiling point	High Pres. energy density	Pres. req.
H_2	9.98 MJ/L	-253 °C	2.96 MJ/L	300 bar
NH_3	15.37 MJ/L	-33 °C	13.77 MJ/L	8.58 bar

Therefore, in order to storage a large enough quantity to power Maui in the absence of an alternative power source it is of clear practical and economic benefit to use ammonia as the medium for long-term energy storage when compared to hydrogen. It is noted that despite the benefits of ammonia over hydrogen storage other methods of energy storage such as pumped hydroelectric are also possible, but outside the scope of this analysis.

1.1.2   List of Design Objectives

The overall objective is to design a synthesis and storage system capable of meeting island energy demand during the absence of wind. This can be broken down into five main design objectives from which to measure success;

1. The process must be of sufficient scale to meet long term average energy demand, whilst meeting the peak demands of the power generation stages.

2. The process should be environmentally beneficial in comparison to traditional power plants.

3. The safety of the design must be prioritised to ensure safe working of the plant.

4. The process must be as economical in order to be financially competitive.

5. The design of the plant must be realistic using technologies that are feasible for the size and lifetime of the plant.

In meeting scale requirements of the process; an initial year long demand requirement for stored energy was calculated in the control and energy matching design process [REFERENCE WILL] this gave both a requirement for the year-long average demand for ammonia and the maximum energy storage requirement during an absence of wind energy. These requirements are shown in Table 2. Using the known efficiencies of the power generation stages and their respective duties an annual demand for ammonia can be calculated using the lower heating value (LHV) of ammonia. Supply-demand matching was also used to calculate the maximum storage required throughout the year, giving the scale requirements for the design process.

As defined by the power demand of Maui, Hawaii the year average power is set to average at a plant output of $36.6 MW$. Accounting for combined generation efficiency in the ammonia-to-power stage of 61.7% this translates into a daily average ammonia output of 227.6 metric tonnes. To account for minor degradation of the process a capacity of 250 tpd will be designed.

Table 2: Design requirements of synthesis stage

Yearly output	Average output	Storage required	Power stage efficiency	LHV NH$_3$
83058 tNH$_3$	227.6 tpd	15000 tNH$_3$	61.7 %	18557 MJ/t

1.2 Review of ammonia synthesis methods

In order to best choose the overall design process a literature review of a number of methods was conducted in order to establish the process that best satisfies the objectives. These can

then be compared with one another to establish the most suitable overall process.

1.2.1 Haber process

The most well-established method for producing ammonia is that developed on in 1913 by Fritz Haber at BASF. This involved the reaction of N_2 and H_2 feed gases over a hetrogenous solid iron catalyst at high temperature and high pressure. The most common catalyst in this process is Fe magnetite. Whilst this process is well established and easily scalable with current production capacities exceeding 3000tpd [3], its low single-pass conversion and large ramp-up time makes it difficult for demand matching, meaning the process is usually run as a continuous process. Despite this a large number of improvements have been made to this process and with the addition of a recycle stream overall conversion rates above 95% are now regularly achieved. Developments into the catalyst composition used in the reactor have led to lower pressure reactors and higher single pass conversion rates. Perhaps the most significant of these has been the development of wüstite as an alternative to magnetite as the iron precursor in the catalyst. This has shown clear advantages in terms of ammonia first pass conversion at lower temperatures and pressures and for similar material promoters[29] [23].

1.2.2 KAAP Ruthenium-based synthesis

A growing competitor to the iron-based synthesis route is an ammonia synthesis production route in which a ruthenium based catalyst is used in place of the iron. Despite known usage in ammonia synthesis since 1917, it was not until 1972 that Ozaki et. al. demonstrated visibly higher activity in ammonia synthesis converters using Ru as an active component. This has led to field of research into its use as a catalyst and in 1992 the development of the Kellogg Advanced Ammonia Process (KAAP) industrial process for Ru-based ammonia synthesis [32]. This process is typically able to operate under significantly lower pressures and feed ratios than iron-based catalysts, meaning a clear economic advantage in terms of reactor and pressure vessel design. The trade-off is the scarcity of ruthenium and thus the significantly higher cost of the catalyst. This can be shown in Table **??** below [22].

The cost of ruthenium being over 50 times greater than that of iron is a huge factor in the cost of the reactor. Furthermore, the poisoning of the ruthenium by high concentrations of

hydrogen can mean the cost of replacing the catalyst is also greater.

Table 3: Comparison of ammonia synthesis catalysts

Catalyst	Availability	Cost (USD/m^3)*	T/ °C	H$_2$/N$_2$ ratio	Energy consumption (Gj/t)
Fe	abundant	4750	350-525	2-3	$\sim$27
Ru	scarce	254100	325-450	under 2	$\sim$27

*converted from CNY data at March 2018 exchange rates

1.2.3 Electrocatalysis

An alternate method of producing ammonia is to use electrocatalysis reaction. This is a non-spontaneous thermodynamic reaction:

$$3H_2O + N_2 \rightleftharpoons 2NH_3 + 1.5O_2 \qquad (K_{eq,298K} = 10^{-120}) \tag{1}$$

This reaction can be powered directly from an electrical source and has shown similar efficiency to established synthesis methods under normal temperatures and pressures [22]. In theory this would be a hugely advantageous design process as it would remove the need for hydrogen electrolysis. In recent years this has been a growing field with research into materials for electro-catalysts and electrolytes, however, whilst developments are being made to increase capacity of such systems to 12.5 t/year, current technology are limited to 0.1 kg/year [11]. A number of obstacles such as low current efficiency and conversion rates make this technology one in need of further development.
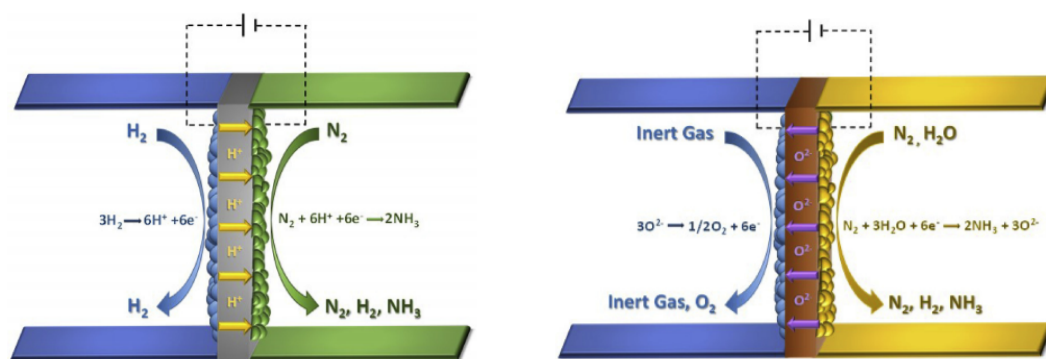

Figure 1: Electrochemical ammonia synthesis - anode (l), cathode (r) [21]

4

1.2.4 Photocatalytic synthesis

Using the same principles of photosynthesis the photocatalytic reaction of nitrogen and water to form ammonia and oxygen can be achieved at room temperature and atmospheric pressure under the addition of solar energy. However, despite ongoing research into this field and a number of photocatalysts available, the scale of this process would currently be unable to meet the ammonia requirement of the plant [22].

1.2.5 Method comparison

Due to the diversity of methods available comparison of these methods will be done using multi-criteria analysis, this is due to the lack of comprehensive data from the electrocatalysis and photocatalysis methods. For simplicity the methods are given a design rating from 1-4 for each of the design objectives. These are then weighted to produce an overall rating for each of the reviewed methods. Safety was not included in this analysis due to the lack of comparative data.

Table 4: Multi-criteria analysis table for reviewed ammonia synthesis methods

| Method	Scale	Environmental	Economic	Feasibility	Total
Fe based Haber	4	3	4	4	**30**
Ru based KAAP	4	3	3	4	29
Electrocatalysis	2	4	2	2	20
Photocatalytic synthesis	1	4	1	1	14
Weighting	**2**	**2**	**1**	**3**	

The Fe-based Haber process was chosen for the synthesis stage.

The weightings were justified with feasibility being the most important due to the need to ensure that only methods able to meet the technological requirements would be used. Whilst new and emerging technologies were considered in the design process priority was given to methods that have been successfully implemented on medium and large scale processes, laboratory condition processes whilst considered were only chosen if there was a clear method in up-scaling to industrial levels and the benefits of doing so were significantly greater than established industrial processes. This was due to the need for reliability of power supply, especially considering the island location of the power plant and the lack of alternative power sources. The next most important considerations were environmental and scale requirements.

This is due to the need to ensure that the methods are able to be sized up sufficiently without the need for large numbers of parallel systems. Environmental was also given a medium weighting of 2 due to its importance in the overall design requirements. Finally, economic was given the lowest ranking on this design process due to the fact that only comparative cost estimates can be found without specific design analysis. The sensitivity of the measurements to changes in score or weighting should also be considered. From the total results only the KAAP process is within 4 points of the Haber total, thus an single unit change in any one rating will only affect the overall optimum if the change was a direct improvement of the KAAP process over the Haber.

1.3 Thermodynamic modelling

In order to make design choices a model for the synthesis of ammonia Haber process must be developed. In order to produce ammonia an exothermic reversible reaction takes place between hydrogen and nitrogen;

$$3H_2 + N_2 \rightleftharpoons 2NH_3 \qquad \Delta h_0 = -92.44 \; kJ/mol \tag{2}$$
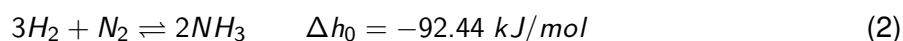
To better understand the nature of the reaction the thermodynamic are be considered in the following sections.

1.3.1 Equilibrium constant

The equilibrium constant K_a for ammonia synthesis was first calculated by Gillespie and Beattie (1930)[12] and is a function of the reaction temperature T.

$$log K_a = -2.69 log(T) - 5.52 \times 10^{-5}T + 1.85 \times 10^{-7}T^2 + \frac{2001.6}{T} + 2.69 \tag{3}$$

This clearly shows a decrease in the concentrations of products as the temperature increases; thus concurring with the Le Chatelier's principle that the equilibrium of reaction will shift to counteract the rise in temperature. This would suggest that a low reaction temperature would favour a high product yield at equilibrium.
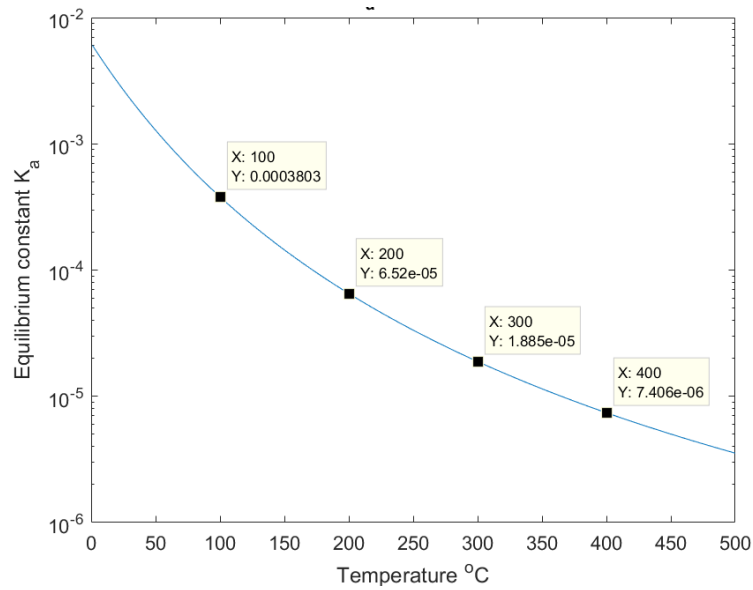
6

Figure 2: Equilibrium constant K_a of ammonia synthesis reaction at varying temperature

1.3.2 Reaction mixtures

When calculating the properties of N_2:H_2:NH_3 streams throughout the system a rule of mixtures is used. Eqn. 4 gives the specific heat of a reaction mixture where x_i are the mole fractions in the stream and $C_{p,i}$ are their respective specific heats.

$$C_{p,mix} = x_{N_2}C_{p,N_2} + x_{H_2}C_{p,H_2} + x_{NH_3}C_{p,NH_3} \qquad (4)$$

The specific heats $C_{p,i}$ can be given by the polynomial temperature correlation, Eqn. 5.

$$C_{p,i} = a + bT + cT^2 + dT^3 \qquad (5)$$

Clearly a Thermodynamic model alone would suggest that to produce high outputs of ammonia the reaction low temperatures should be chosen. However, this model is insufficient without also considering the rate at which this reaction would occur.

1.4 Mechanism and Kinetics

For a large scale process such as the Haber process with a large product output the rate at which the reaction occurs is an significant limitation on the product output of the plant. This

Table 5: Specific heat coefficients [26]

Coef.	N_2	H_2	NH_3
a	28.9	29.11	27.568
b	$-0.1571 * 10^{-2}$	$-0.1916 * 10^{-2}$	$2.5630 * 10^{-2}$
c	$0.8081 * 10^{-5}$	$10.4003 * 10^{-5}$	$0.99072 * 10^{-5}$
d	$-2.873 * 10^{-9}$	$-0.8704 * 10^{-9}$	$-6.6909 * 10^{-9}$

is due to the fact that over a limited reaction time the reactants do not have sufficient time to reach a thermodynamic equilibrium.

1.4.1 Reaction mechanism

The reaction mechanism of the ammonia synthesis stage was key in understanding the kinetics of reaction, determining the rate of reaction and the effectiveness of a catalyst. The mechanism for the synthesis reaction is shown in Fig. **??** [18].

Where $*$ denotes the formation of an adsorption site. Experimental studies have found the adsorption of nitrogen to be rate determining in this process leading to an understanding of the microkinetics of the rate of reaction. This is due to the energy required to break the strong N_2 triple bond.
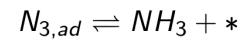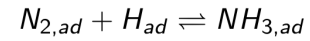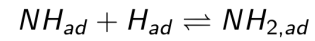
$$H_2 + * \rightleftharpoons 2H_{ad}$$
$$N_2 + * \rightleftharpoons N_{2,ad}$$
$$N_{2,ad} \rightleftharpoons 2N_{ad}$$
$$N_{ad} + H_{ad} \rightleftharpoons NH_{ad}$$
$$NH_{ad} + H_{ad} \rightleftharpoons NH_{2,ad}$$
$$N_{2,ad} + H_{ad} \rightleftharpoons NH_{3,ad}$$
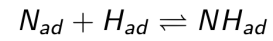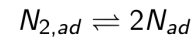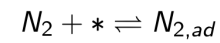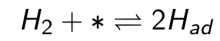$$N_{3,ad} \rightleftharpoons NH_3 + *$$

Figure 3: Synthesis mechanism

1.4.2 Rate of reaction

Numerous models [1] for the synthesis rate of reaction r have been established, however, the most widely used is the Temkin equation [14]. Since its discovery a number of different forms of the equation have now been developed. This analysis uses the Dyson and Simon form for its simplicity and the limited experimental data required to simulate results [7].

$$r_{NH_3} = K_2 \left[K_a^2 \times f_{N_2} \left(\frac{f_{H_2}^3}{f_{NH_3}^2} \right)^{\alpha} - \left(\frac{f_{NH_3}^2}{f_{H_2}^3} \right)^{\alpha-1} \right] \tag{6}$$

Where the rate is a function of the fugacities f, the well-known equilibrium constant K_a, empirical constant α and K_2 defined by the Arrhenius law: where k_20 and E_2 are found experi-

mentally and R is the gas constant.
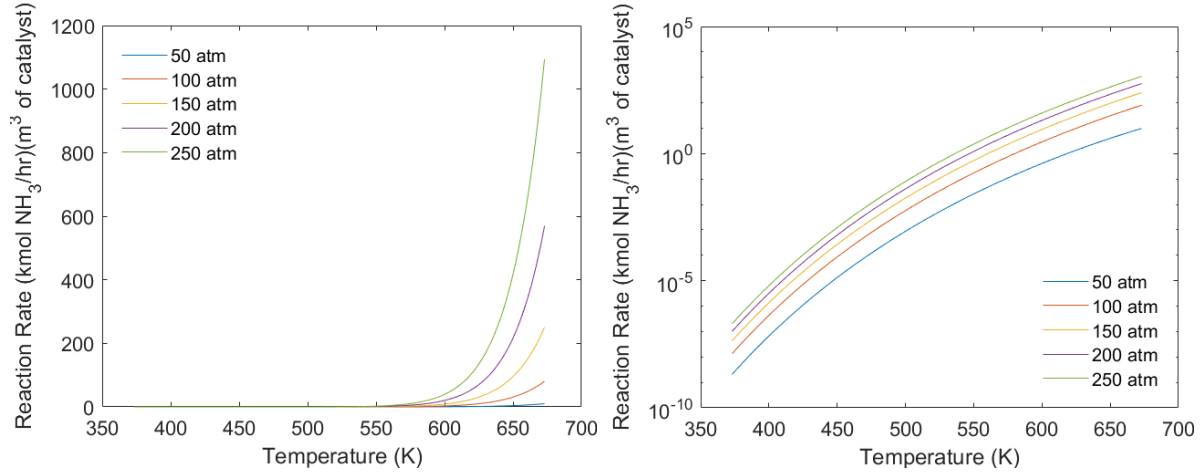
$$K_2 = k_{20}e^{-E_2/RT} \tag{7}$$

Figure 4: Reaction rate of ammonia synthesis

Figure **??** shows a significant increase in the rate of reaction as temperature increases, thus whilst the thermodynamic equilibrium decreases with temperature the rate of reaction increases. It is clear that as pressure increases the rate does also. Due to the NH_3 term in the denominator of the Temkin equation it is undefined when no ammonia is present. Clearly this does not follow the thermodynamic principles of a reverse reaction. Thus in practice a small amount ($\leq$1%) of ammonia was included in the initial reactants and the reactor will be run at steady state conditions.

1.4.3 Fugacities

The fugacities f_i of the respective gases can be calculated from the pressure P and mole fraction of ammonia Z using:

$$f_{N2} = P\gamma_{N_2}\frac{a}{3\delta}(1 - b_2 Z) \tag{8}$$

$$f_{H2} = P\gamma_{H_2}a(1 - b_1 Z) \tag{9}$$

$$f_{NH_3} = P\gamma_{NH_3} \times Z \tag{10}$$

Where $a = \frac{3\delta}{3+1}$, $b_1 = \frac{i_0+0.5+(0.5/\delta)}{1-i_0}$, $b_2 = \frac{i_0-0.5+1.5\delta}{1-i_0}$ and 3δ is the H/N ratio. Fugacity

9

coeffiecients γ can be calculated using the Cooper (1967) and Newton (1935) expressions given as:

$$\gamma_{N_2} = 0.93432 + 0.3102 \times 10^{-3}T + 0.2959 \times 10^{-3}P - 0.2707 \times 10^{-6}T^2 + 0.4775 \times 10^{-6}P^2 \quad (11)$$

$$\gamma_{H_2} = exp\{e^{-3.840T^{0.125}+0.541}P - e^{-0.126T^{0.5}-15.98}P^2 + 300[e^{-0.01190T-5.94}](e^{-P/300} - 1)\} \quad (12)$$

$$\gamma_{NH_3} = 0.1439 + 0.2029 \times 10^{-2}T - 0.4488 \times 10^{-3}P - 0.1143 \times 10^{-5}T^2 + 0.2761 \times 10^{-6}P^2 \quad (13)$$

The sensitivity of the fugacity coefficients to temperature can be seen on figure **??**. Showing that as temperature decreases and pressure increases the behaviour of gases becomes increasingly non-ideal.
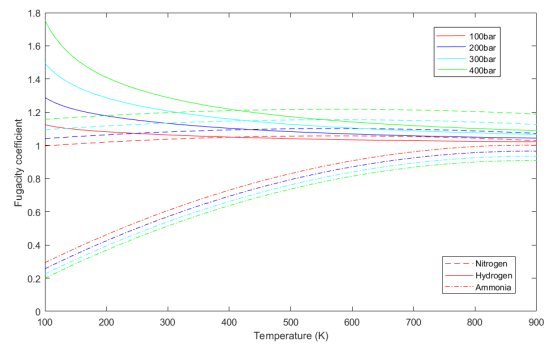

Figure 5: Variation of fugacity coefficients with temperature

1.4.4 Modelling

The kinetics were implemented in ASPEN using a Langmuir-Hinshelwood-Hougen-Watson (LHHW) model, simulating the surface mechanisms during reaction. This is commonly used modelling heterogeneous reactions with a solid catalyst and fluid reactants. For ASPEN simulation the model must be given in the form [30]:

$$\text{Rate} = \frac{\text{(Kinetic factor)(Driving force)}}{\text{(Absorption)}} \quad (14)$$

In this form and using the Dyson and Simon form of the Temkin equation the absorption term can be set to unity and the kinetic factor to K_2, giving a driving force expression:

$$\text{Driving force} = K_a^2 \times f_{N_2} f_{H_2}^{3\alpha} f_{NH_3}^{-2\alpha} - f_{NH_3}^{(2\alpha-2)} f_{H_2}^{(3-3\alpha)} \quad (15)$$

Using the experimental values for k_{20} and E_2 in Eq. **??** to calculate K_2 and then the Gillespie and Beattie equation (Eq. **??**) to calculate K_a and an experimental value of $\alpha = 0.5$ a kinetic model for the reaction was formed. Initial simulations of this model in a PFR reactor in aspen at a first approximation of industrial conditions (p=100bar T=400°C) giving a first pass conversion

of $\approx 25\%$ NH_3.

1.5 Catalyst

In modelling the rate of reaction Dyson and Simon accounted for the flow of reactants through a reactor. In order to account for the presence of a solid catalyst an effectiveness factor ξ_c was used such that an effective rate ($r_{eff} = \xi_c r_{NH_3}$) through the reactor could be calculated using the following assumptions [7]; The catalyst particles can be considered as spheres. The diffusion coefficients of each component are independent of position within a particle, particles are isothermal and Knudsen diffusion is not experienced. Giving the equation:

$$\xi_c = \frac{\text{(molar flux of component i across surface)} \times \text{(surface area of catalyst pellet)}}{\text{(vol. of catalyst pellet)} \times \text{(rate of formation of component i at surface)}} \quad (16)$$

Throughout the past 100 years of an Fe-based magnetite (Fe_2O_3) precursor with a variety of oxidic promoters have been the principal catalyst used industrially in ammonia synthesis [22]. However, over the past few decades a number of additional catalysts have been developed. These involve the use of a various other materials as promoters including ruthenium

Table 6: Wüstite catalyst [29]

A301 particle size	1.5-3.0mm
Bulk density	3.25 g/cm^3
BET surface area	16.6 m^2/g
K_{20}	0.874 x 10^{16}
E_2	44.9 kcal/mol

and bimetallic nitrides. These were considered during the initial design of the plant due to their higher yields of ammonia at reduced pressures. This was mainly due to both the high cost and limited availability of ruthenium. Considering the island location of the power generation facility the availability of resources was a key factor in the choice of catalyst. On balance, the additional cost of these materials are substantially higher than iron and thus greatly increase both the initial capital costs of the plant but also the running costs of the plant due to the increased material costs. Thus an alternative wüstite ($Fe_{1-x}O$) iron catalyst was chosen for the ammonia synthesis stage. This was chosen due to the increased reaction rate at lower operating pressure than the traditional magnetite promoter thus reducing the pressure needed for the reactor and thus the capital costs required. The catalyst in use will be the A301 catalyst manufactured by Shangyou Catalyst Co. Ltd.

Table 7: A301 Catalyst composition

Compound	Fe oxide	Al_2O_3	K_2O	CaO	Others*
A301 (%)	93.0	2.7	0.8	2.8	0.7

*Impurities in raw material

1.6 Reactor design

The synthesis reactor is central to the design of the process as it is within here that the synthesis reaction takes place. In order to maintain close to optimum conditions a two bed reactor with intercooling between them was chosen. This enables the products of the first bed to return to a lower temperature before entering the second stage.
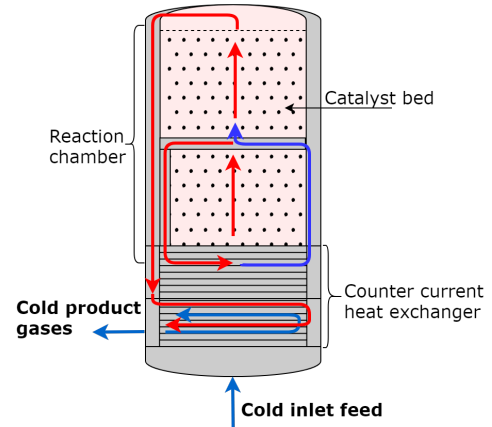
1.6.1 Reactor sizing

Figure 6: Two stage reactor

The reactor consists of two reactor stages with inter-stage indirect cooling. Both reactor inlet stages are designed as fixed bed reactors with an even catalyst spacing throughout. The overall volume of the reactor V, can be given by equation **??**: where r is the rate of reaction, ρ_{cat} is the packing density of the catalyst and $\dot{m}$ the mass flow rate [3].

$$V = \frac{\dot{m}}{1000\rho_{cat}r} \tag{17}$$

Table 8: Reactor sizing

Reaction rate r	ρ_{cat}	$\dot{m}_{NH_3}$	V	L_T	D_T
$1.3838 * 10^{-4} \ \frac{kg_{NH_3}}{s^{-1}kg_{cat}^{-1}}$	3.25 kg/L	3.22 kg/s	7.16 m^3	2.74 m	1.83 m

1.6.2 Dimensions and Pressure Drop

Pressure drop across a reactor can be calculated using the Ergun equation [10]:

$$\frac{\Delta p}{L} = \frac{150\mu(1-\epsilon)^2}{D_p^2 \epsilon^3} v_s + \frac{1.75(1-\epsilon)\rho}{D_p \epsilon^3} v_s^2 \tag{18}$$

where Δp is the pressure drop across the length L of the bed, μ is the fluid viscosity, ϵ is the void space in the bed (taken as $\epsilon = 0.5$ [10]), ρ is the density of the fluid, D_p is the particle diameter and v_s is the superficial velocity of the fluid where $v_s = \frac{Q}{A} = \frac{\text{volumetric flow rate}}{\text{bed cross sectional area}}$.

Table 9: Reactor dimensions and pressure drop

Reactor bed	Volume m^3	Length m	Diameter m	Thickness mm	Δp atm
1	3.28	1.25	1.83	47.0	4.30
2	3.91	1.49	1.83	47.0	4.08

Modelling the outlet temperature against reactor length in figure **??** for a single bed with an input temperature of 400 °C and a diameter D_1 = 1.83 m shows a change in the reactor profile up to L_1=1.25 m after this point increasing the reactor length no longer increases the NH$_3$ yield thus this was chosen as a suitable length for the first stage. Using this first stage design a second bed could be subsequently designed; a larger bed was required to optimise ammonia yield. Simulating the reactor bed on ASPEN an optimum length of D_2=1.82 m and L_2=1.49 m was chosen as after this point there was no significant increase in performance with reactor length, giving a first pass conversion of 34.2% [8].
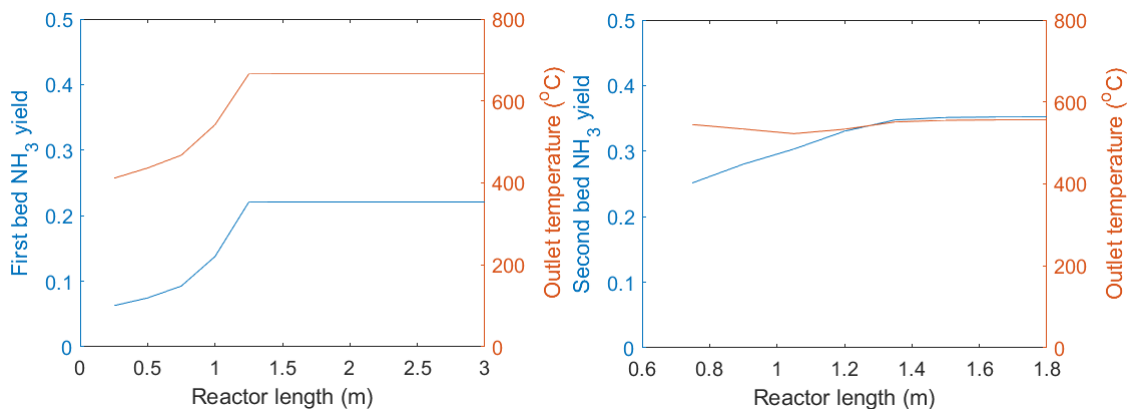

Figure 7: First (l) and second (r) reactor temperature and yield profile with length

Furthermore, under a reactor pressure of 150 bar (*see optimising operation and control*) the thickness of the walls must be sufficient to withstand the high internal pressures of reaction.

1.6.3 Material selection

In order to calculate the thickness of material required the internal reactor forces must be measured, as must the operating temperatures. Simulating shows the peak temperature of normal operation of the reactor remains below 700°C. Therefore assuming a material with a melting point significantly higher than this would be required. Due to the corrosivity of NH_3 to a number of metals high-yield steel was chosen as the material for construction of the vessel.

Table 10: Properties of high yield steel [16]

Density	Melting point	Yield stress	Ultimate tensile strength	Cost
7850 kg/m^3	1500°C	400 MPa	600 MPa	$896/ton [24]

To ensure the reactor material can withstand the reactor pressures it must both withstand the hoop and longditudinal stresses within the reactor such that:

$$\frac{\sigma_{yield}}{S.F.} \geq \sigma_L = \frac{PD}{4t} \text{ and } \frac{\sigma_{yield}}{S.F.} \geq \sigma_H = \frac{PD}{2t} \tag{19}$$

where a safety factor of 2 is taken. This gives the condition that for high yield steel $t \geq 46.9 \ mm$, the thickness of the vessel is taken to be $47 \ mm$.

CHECK LEAK BEFORE BREAK CONDITION

1.6.4 Heat exchanger

For the two stage reactor design intermediary cooling is key factor in ensuring the exothermic synthesis reaction does not result in an unwanted temperature increase, thus shifting the equilibrium of reaction further towards the reactants. There were two main methods considered in literature. These were direct quench cooling and heat exchanger indirect cooling.

Quench cooling Direct quench cooling involves the addition of cold feed mixtures during the reactor stages in order to reduce the reactor temperature at each stage. This means that only a fraction of the total feed enters the first reactor stage. Indirect cooling Indirect cooling involves a heat exchanger passing the hot product gases past the cold feed gases in order to raise the temperature of the feed gases. This means the entire feed stream passes through all reactor stages and thus the time in the reactor is maximised. Design The chosen method for

cooling configuration was the indirect cooling \{}caption{First and second reactor temperature and yield profile with length} due to the maximisation of reaction time. This is supported by empirical analysis [28]. The heat exchanger used in the reactor is a counter-current heat exchanger with steady state heat transfer. From this it is possible to derive an energy balance equation [19];

$$\frac{dT_c}{dx} = \frac{UA}{\dot{m}_i C_p^i L}(T_h - T_c) \tag{20}$$

$$\frac{dT_h}{dx} = \frac{UA}{\dot{m}_o C_p^o L}(T_h - T_c) \tag{21}$$

In which T_c and T_h are the respective cold inlet and hot outlet streams. A is the area for heat transfer to occur and U is the overall heat transfer coefficient of the heat exchanger $(290.35 \text{Wm}^{-2}K^{-1})$[9], whilst C_p are the specific heat capacities for the respective inlet and outlet streams of gas mixtures (Eqn. **??**) and $\dot{m}$ are the mass flow rates of the respective streams. Along a heat exchanger of length L where x is the relative position along it. If we then assume $\dot{m}_i c_p^i$ is equal to $\dot{m}_o c_p^o$ and similarly $\frac{UA}{\dot{m}_i c_p^i}$ does not depend on x; then the above expressions can be simplified in order to give the temperature at the reactor inlet and outlet:

$$T_r^i = \frac{T_i + \frac{UA}{\dot{m}_i C_p^i} T_r^o}{1 + \frac{UA}{\dot{m}_i C_p^i}} \tag{22}$$

$$T_o = \frac{T_r^o + \frac{UA}{\dot{m}_i C_p^i} T_i}{1 + \frac{UA}{\dot{m}_i C_p^i}} \tag{23}$$

The aim of the heat exchanger is twofold. The first of these is to heat up the feed of the product gases to a significantly high temperature to allow for a suitable rate of reaction. This is done by running the hot product gases in counter current to the feed gases. The second use of the heat exchanger is in a two-stage reactor system the heat exchanger acts as an intermediary coolant for the product gases. This brings the temperature down to one in which the reaction equilibrium maintains a increased fraction of ammonia products.

1.7 Additional units

1.7.1 Separator

In order to remove the fraction of ammonia from the product mixture, the relatively high boiling point of ammonia was used to remove liquid ammonia at high pressure and low temperature in a separator. This separates liquid droplets from gas particles by using gravity separation to allow the gaseous products to leave from the top outlet whilst liquid ammonia is removed from the bottom outlet in a vertical separator.
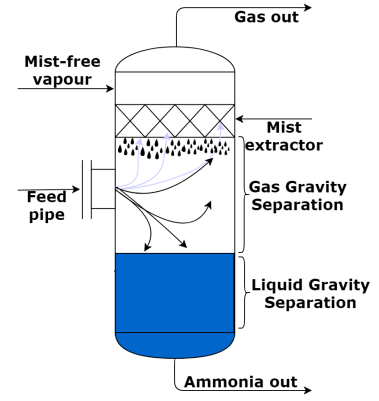

Figure 8: Vertical separator

To separate liquid ammonia from the product gases The Souders-Brown design equations were used to equate the drag force F_D exerted by gas flow to the gravity force of the droplet weight F_G [6] [17]. Such that assuming plug flow $F_D = F_G$. Substitution of expressions for the forces on a spherical droplet give the maximum gas velocity, V_{Gmax} using the Souders-Brown method [34];

$$V_{Gmax} = K_s \sqrt{\left(\frac{\rho_L - \rho_G}{\rho_G}\right)} \; when \; K_s = \sqrt{\left(\frac{4gD_P}{3C_D}\right)} \tag{24}$$

$$D_{min} = \sqrt{\left(\frac{(4/\pi)q_a}{F_G V_{Gmax}}\right)} \tag{25}$$

Where K_s is found experimentally. Using a mist extractor - a horizontal wire mesh pad in a vertical separator used to coalesce the liquid into droplets large enough to drop from the mesh pad - gives $K_s = 0.12$. For a length/diameter ratio of 4/1 to reduce the material required in construction. And using a industrial standard HY-80 steel the separator can be modelled as a thin walled pressure vessel to calculate the required wall thickness of the tank [16].

$$\sigma_{yield} = \frac{pr}{t} \tag{26}$$

For an internal pressure of 140 bar, known material and dimensions of the separator can be sized.

Table 11: Separator design summary

K_s	V_{Gmax}	D_{min}	F_G	H	Vol
0.12	74kW	0.594 m	1	2.296 m	0.636 m^3

1.7.2 Compressor

In order to obtain the high operating pressures required for ammonia synthesis centrifugal compressors are used both in the feed streams and in the reactor inlet stream. The feed compressor is used to raise the pressure of the feed gases to the pressure of the recycle stream. Whilst the reactor inlet compressor raises the pressure to account for the pressure drop across the reactor. In this analysis the compressors are assumed to be driven by electric motors, however, turbine powered compressors are also possible, had the gas turbine generator been run continuously for power generation, this would also have been considered. For an isentropic compressor the total output temperature can be calculated from Eqn. **??** [26].

$$T_{out} = T_{in} \left[\left(\frac{P_2}{P_1} \right)^{\frac{1}{N}} \right]^{\left(\frac{n-1}{n} \right)} \tag{27}$$

The total compression power required $\dot{W}_{fluid}$ for the fluid is given by Eqn. **??**

$$\dot{W}_{comp} = \frac{\dot{W}_{fluid}}{\eta_{comp}} = \frac{1}{\eta_{comp}} TN \frac{n}{n-1} R\dot{m} \left(\left[\left(\frac{P_2}{P_1} \right)^{\frac{1}{N}} \right]^{\left(\frac{n-1}{n} \right)} - 1 \right) \tag{28}$$

Where T is the input temperature, N is the number of compressor stages, n is the polytropic exponent, R the specific gas constant, $\dot{m}$ is the mass flow rate and P_1 and P_2 are the respective inlet and outlet pressures. η_{comp} is the overall compressor efficiency which the product of mechanical and isentropic efficiencies such that $\eta_{comp} = \eta_{is}\eta_m$. Standard efficiences of centrifugal compressors are taken as $\eta_{is} = 0.85$ and $\eta_m = 0.95$ [28].

Table 12: Combined compressor power requirements of plant

Compressor	T_{in} (K)	n	P_2/P_1	N	$\dot{W}_{fluid}$	$\dot{W}_{comp}$
1	298	1.40	25	2	1084 kW	1342 kW
2	513	1.40	5.6	2	892 kW	1104 kW
3	565	1.40	1.07	1	77 kW	95 kW
Total					**2053 kW**	**2541 kW**

The total cooling power, $\dot{Q}$ can be found in order to size the intercooling heat exchangers: where $C_{p,mix}$ is found from equation **??**.

$$\dot{Q} = \dot{m}(N-1)(T_{out} - T_{in})C_{p,mix} \tag{29}$$

1.7.3 Purge

In order to limit the build-up of inert gases within the synthesis loop, a fraction of the recycle loop is purged. However, due to the cost of obtaining feed gases it is beneficial to keep the purge fraction small. After simulating a number of purge fractions on ASPEN a fraction of 5% of the recycle stream was chosen. This purge stream is comprised of mostly H_2 and N_2 feed gases. Considering the high energy requirement of the electrolyser hydrogen recovery of this stream is in both environmental and economic interest. For this stage there are two main methods; membrane technology and cryogenic separation. With the former generally requiring a lower initial investment whilst the latter provides a greater energy efficiency [27]. Further economic evaluation of this process is outside the scope of this design.

1.8 Ammonia storage

Storage of liquid ammonia product is vital in matching the supply and demand sides of the plant. Thus the scale of this storage must be one of the largest stores in the plant. Liquid ammonia has a boiling point of -33.3°C at atmospheric conditions, however, this can be increased by pressure storage. This requires a compromise to be made between low temperatures and high pressures in which to store ammonia. A review of current large-scale ammonia storage methods (Bartels,2008)[4] highlights the main trade-off between high pressure and low temperature storage being the high capital cost of building high pressure vessels against the increased energy requirements and thus running costs of maintaining low temperature storage. As calculated in [REFERENCE THE DEMAND/SUPPLY PROFILING] the maximum capacity for required ammonia storage is calculated to be 15000 tonnes at maximum capacity.
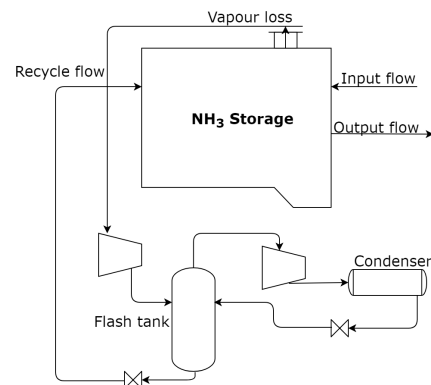

Figure 9: Cold NH_3 storage cycle

18

1.8.1 Low temperature storage

Storage of NH_3 at low temperature and ambient pressure is commonly used for large scale storage due to higher ammonia/steel ratio and thus a reduction in capital cost. At atmospheric pressure approximately 43 tonnes of ammonia can be stored per tonne of steel. This massively reduces the capital cost on steel. Despite this other factors must also be considered, mainly boil-off rate due to heat transfer from the environment. The mass of evaporated ammonia and thus the boil-off rate is given as;

$$NH_{3evap} = \frac{\dot{Q}}{\Delta H_{vap}} \tag{30}$$

$$\text{Boil-off (\%)} = \frac{NH_{3evap}}{NH_{3storage}} \tag{31}$$

This is typically below a conservative estimate of 0.1% per day [5]. Giving a maximum boil-off of 15 t/d. Using an ammonia refrigeration cycle system for 15000 tonnes a storage tank of at least 21.997×10^3 m^3 would be required (density of liquid ammonia, $\rho_{NH_3(l)}$=681.9 kg/m^3)[15].

1.8.2 High pressure storage

Pressure storage does not suffer from evaporation losses or cooling costs. However, it is limited by its structural mechanics and this material used for construction of the pressure vessel. To increase capacity more vessels are required. Bartels shows that in order to store ammonia at an ambient temperature of 20°C, a pressure of 8.58 bar would need to be maintained. However, the limiting size of a steel pressure vessel is calculated to be approximately 270t. The recommended ratio is about 2.8 ton NH_3 stored for every tonne of steel.

1.8.3 Design

Due to the scale of the process high pressure storage would require at least 55 pressure vessels with over 5000 tonnes of steel thus cold storage is a preferred option due to environmental and economic benefits.

In order to minimise the heat transfer the surface area/volume ratio of the storage tank must be minimised. Despite the optimal ratio of a spherical tank the 3d nature of the shape would

Table 13: Comparison of ammonia storage methods

Ammonia Storage - 15000 tonnes required		
Properties	High pressure	Low temperature
NH$_3$ Energy density (MJ/L)	13.77	15.37
Ammonia/Steel ratio	2.8	43
Pressure required (bar)	8.58	Atmospheric
Temperature required (^{o}C)	20	-33.3
Storage efficiency	100%	96.3%
Tanks required	55	1
Steel required (tonnes)	5357	349

cause significant structural issues in building a sufficiently large container, thus a 3d projection of a 2 dimensional shape is preferred for vertical support. The optimal shape of this design is a cylindrical storage tank. For a maximum volume of 21.997×10^3 m^3 the optimum radius/height ratio is $\frac{h}{r} = 2$ giving a radius, r = 15.184m and height, h = 30.38m steel containers. Insulated double containment tanks are used to minimise heat transfer and to ensure toxic vapours are not released in the case a rupture. The outer tank is made from concrete. Estimation of the hydrostatic pressure at the bottom of the storage container can be given by the equation:

$$P_h = \rho g h \tag{32}$$

In the case of ammonia the pressure on the bottom of the tank would be 203.144 MPa of additional pressure. Thus a suitable steel thickness would have to be chosen to withstand this.

Designing the refrigeration system using the compressor design equations and with a flash tank liquid holdup time of 10m the condenser can be sized using [26]0;

$$\text{Area} = \frac{\dot{m}H}{U_{cond}T_{LMTD}} \tag{33}$$
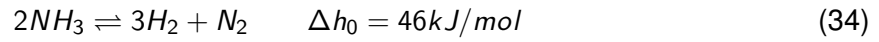
Where H is the specific mass enthalpy.

Table 14: Storage refrigeration cycle design summary

Flow rate $\dot{m}$	Compressor power	Flash volume	Condenser area
0.17 kg/s	74kW	0.31 m^3	69.7 m^2

1.9 Ammonia cracker

In order to produce feed gases for the gas turbine the liquid ammonia must first be decomposed into N_2 and H_2 in the endothermic reaction [20].

$$2NH_3 \rightleftharpoons 3H_2 + N_2 \qquad \Delta h_0 = 46kJ/mol \qquad (34)$$

This requires the addition of heat due to the endothermic nature of the reaction and thus must be conducted in a furnace with a nickel catalyst to achieve the conversions required to decomposition.

Due to the high peak demands of the 3 gas turbines a small amount of storage of the cracked gas is stored. This is done to reduce the peak requirement of the cracker. The standard capacity of a industrial cracker is 1000 m³/h at operating conditions the plant would require 26 SINCE-GAS ANH units at a cost of \$260000 per unit [33].

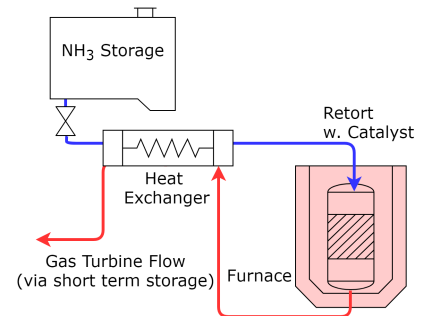Figure 10: Ammonia cracker flow network

Table 15: Ammonia cracker design requirements

Peak NH_3 mass flow demand	32.815 kg/s
Average NH_3 mass flow rate required	0.1648 kg/s
Ramp-up time of SOFC	0.5h
Maximum theoretical capacity required	59067 kg/SOFC ramp-up
Minimum turbine down-time	2h
Capacity requirement of cracker	5.469 kg/s
Cracked gas storage requirement	49.223 ton
Total cost of cracker	\$6,760,000
Operating pressure	0.5 - 1.0 bar

1.10 Simulation, optimisation, and control

This section addresses the methods used in modelling, optimising and controlling the process in order to achieve peak operating conditions.

1.10.1 MATLAB modelling

MATLAB was used to initialise the model and plot the changes of reactor conditions. This was especially useful at visualising relationships between a small number of variables over a variety of conditions.

1.10.2 ASPEN simulation

In order to optimise the pressure and temperature conditions, a number of simulation conditions were trialled using ASPEN plus. Thus measuring the first pass ammonia yield of the reactor at varying operating conditions. Plotting these results shows a peak in NH_3 yield at a temperature of 400 °C. Increasing pressure clearly is shown to increase yield, however, above a pressure of 150 bar the there is a fall in the rate of increase. From this analysis the reactor operating point was set at 150bar and 400 °C. This was due to the desire to maximise first pass NH_3 yield whilst keeping the plant as economically viable as possible. The flow model used for simulation can be seen in Figure **??**.

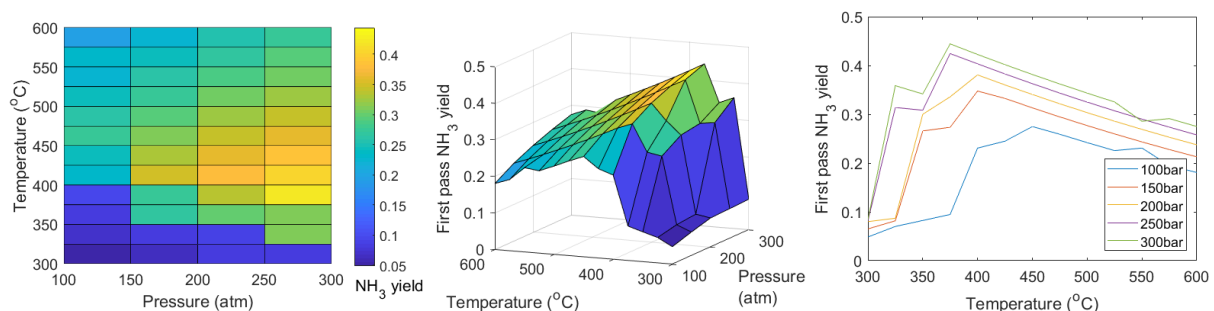Figure 11: Ammonia single pass yield as function of temperature and pressure

1.10.3 Model limitations

There are a number of limitations of the overall model for the process, the most of important of these are summarised here.

- The lack of a comprehensive process simulation on ASPEN. This is due to the difficulty in matching variable demand data into the simulation. Thus only the synthesis stage was simulated.
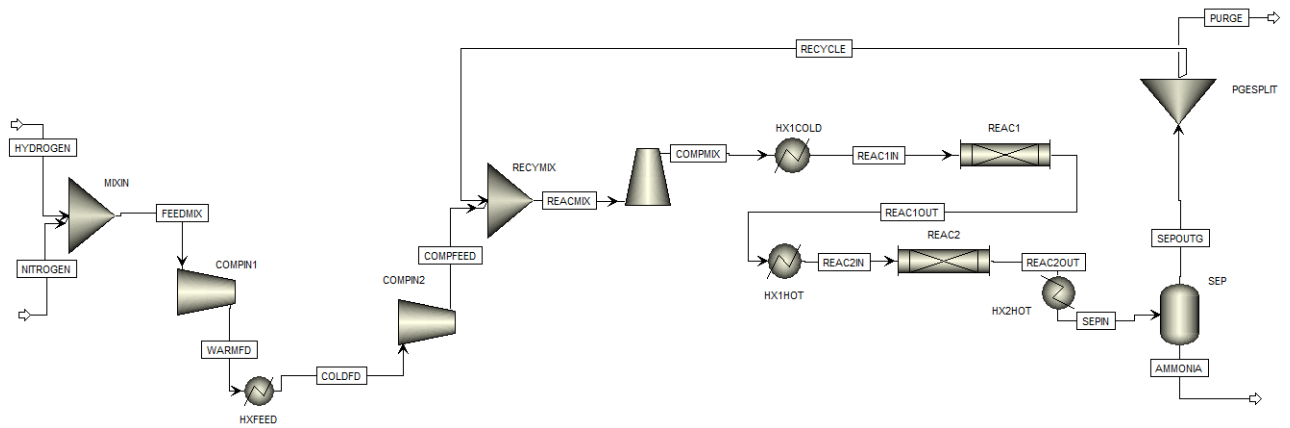
Figure 12: ASPEN model of synthesis reaction

- The simulation limitations, a number of stages - in particular the ammonia cracker was limited to a rudimentary design.

- We have conveniently assumed steady state operation without analysis or process ramping that may be required for maintenance.

- The model assumed that yearly average supply was constant and gave no consideration to a growing power demand.

1.10.4 Plant control

The ammonia synthesis process is designed to run at steady state conditions and thus the need for plant control on this process is limited. The overall plant supply/demand matching control has been designed in REFERENCE WILL HERE. However, to ensure safe operating temperatures of the reactor an emergency quench feed can be used to lower the reactor feed temperature. Above a threshold safe output temperature of T_{th}=700 °C a control feed is used to lower the reactant temperature. Energy required for cooling per °C required is:

$$\frac{\dot{Q}}{T} = \dot{m}C_{p,mix} \tag{35}$$

A full control system for the ammonia synthesis process using quench cooling is given by Araujo [2]. However, in this design only
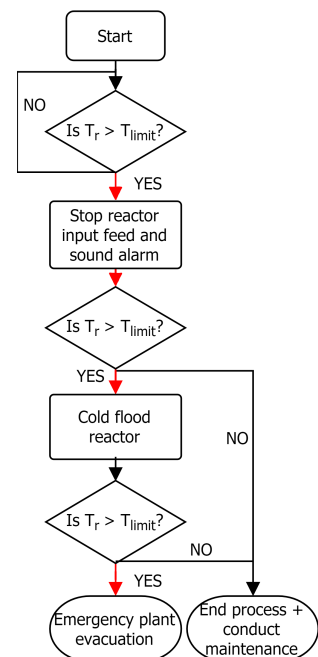

Figure 13: Synthesis reactor emergency control system

the emergency reactor control system is considered (Fig. **??**).

1.11 Economic, Sustainability and Safety Assessment

In this section only the capital cost assessment for the design stage was conducted. For plant operating costs see section ZZZREFERENCE HERE.

1.11.1 Capital Cost

An economic analysis of the ammonia synthesis and storage system requires an assessment of the costs associated with each stage of the design. In this analysis module factor costing method was used for the costing of components [31]. Where the purchasing cost C_p^o of equipment in USD is given by the equation [3];

$$log_{10} C_p^o = K_1 + K_2 log_{10}(A) + K_3 (log_{10}(A))^2 \tag{36}$$

Where K_1, K_2, K_3 are defined in Table **??**. Thus the bare module cost C_{BM} (direct and indirect costs from purchase and installation) can be calculated from:

$$C_{BM} = C_p^o F_{BM} = C_p^o (B_1 + B_2 F_M F_P) \tag{37}$$

Where F_M and F_P are the respective material and pressure factors and B_1, B_2 are constants defined by design. Data for these constraints can be found in data sets and ASME tables [31]

1.11.2 Process Sustainability

Whilst the overall system sustainability is covered later in this report. The ammonia synthesis and storage stage of this project has been one in which no external inputs have been used besides the environmentally produced hydrogen and nitrogen in order to make liquid ammonia. In addition to this recycling the outlet streams has in some cases increased overall output efficiency by a factor of 3, whilst reducing waste streams.

Table 16: Cost summary of all components within the ammonia synthesis and storage process

Component	A	K_1	K_2	K_3	C_p^o	F_{BM}	C_{BM}
Synthesis loop							**$4.017 m**
Reactor	7.16 m^3	4.0152	0.4485	0.1074	$ 0.005m	118.18	$0.591 m
Compressors	2541 kW	2.2897	1.3604	-0.1027	$0.538 m	5.80	$3.120 m
Separator	0.636 m^3	3.4974	0.4485	0.1074	$0.003 m	118.18	$0.306 m
Storage							**$4.705 m**
Steel Tank	21997 m^3	4.8509	-0.3973	0.1445	$0.708 m	4.5	$3.186 m
Concrete Tank	26699 m^3	4.8509	-0.3973	0.1445	$0.839 m	1.5	$1.259 m
Compressor	74 kW	2.2897	1.3604	-0.1027	$0.030 m	4.4	$0.132 m
Condenser	69.2 m^2	4.0336	0.2341	0.0497	$0.043 m	2.99	$0.129 m
Cracker							**$6.760 m**
Cracker	-	-	-	-	$6.760 m	-	$6.760 m
Total	-	-	-	-	-	-	**$ 15.482 m**

Table 17: HAZOP analysis of synthesis stage

Line	Dev.	Cause	Consequences	Action
Reactor	No	Valve stuck/blocked	Rapid temperature change, Catalyst damage, Reaction rate fall.	Measure temperature with a thermocouple and flow rate continuously with alarm and shut down system, catalytic testing.
	Less	Low output concentration, Reactor leakage, Temperature fall	Release of reactants, fall in output. Explosive ammonia/air mixture.	Measure concentrations of gases outside of the reactor to detect any leakage of reactants. Catalyst replacement.
	More	Overpressure Overtemperature	Vessel failure, release of reactor gases.	Pressure and temperature sensors and warnings, complete shutdown at system before critical level reached. Alarm system in place.
H. Exch.	No	Valve stuck, blockage	Pipe burst - gas leak	Flow path redundancy in HX.
	Less	Low heat exchange - damage to surface plate, low flow rate.	Fall in output, damage to HX.	Thermocouple to measure temperature profile of flow. Regular maintenance.
	More	High flow rate, high temperature	Overheating of reactor.	Measure flow temperature. Regular maintenance.
Compr.	No	No flow - pump blockage, no power supply, complete pressure loss - leak of compressor	Gas leak into atmosphere, reduction in reaction conversion	Gas monitoring outside chamber, regular maintenance.
	Less	Low compression level - low power supply/blockage in system	Inefficient operation, damage to pump.	Filter of feed, flow rate and pressure monitoring.
	More	Overcompression, power surge, control failure, high flow rate	Damage to compressor pump, pipe rupture.	Power buffer systems. Warning and detection alarms.
Separ.	No	No output flow - separator leak	No ammonia output, gas leak	Continuous monitoring of pressure, temperature and flow rates. Regular inspection.
	Less	Temperature too high	Mesh damage, low yield.	Regular stream testing. Periodic inspection.
	More	Temperature too low	Power wastage in cooling.	Thermocouple to measure vessel temperature.
Storage	No	No	Failure power generation stages	Monitoring of storage levels, low storage warning.
	Less	Refrigeration failure of vessel	Building up of pressure - burst vessel	Leak before burst design of storage tank. Pressure relief valve.
	More	Buildup of pressure in container - failure of gas release valve	Vessel failure/bursting. Explosive ammonia/air mixture.	Redundancy in release valves, regular inspection. Pressure monitoring inside vessel.

1.12   Section Results and Conclusion

1.12.1   Results

During the final design iteration of the synthesis stage a first pass conversion rate of 34% can be achieved after optimization. This is achieved at a pressure of 150bar and a reactor inlet temperature of 400 °C. Figure **??** shows the final stage ammonia synthesis stage ASPEN flow diagram.

Table 18: Design summary

NH$_3$ production rate	257 tpd
NH$_3$ storage capacity	15000 t
Capital cost of process	$15.5 m
Single-pass NH$_3$ conversion	34%
Overall NH$_3$ conversion rate	96%
Operating pressure	150 bar
Operating temperature	400 °C
Synthesis pressure	1 bar
Synthesis temperature	-33 °C

The ammonia synthesis, whilst a well established process requires careful design and optimisation of the process due to the specific design requirements. The use of ASPEN and MATLAB has allowed for the creation of a dynamic modelling system that has enabled the conversion rate of ammonia within the reactor to be optimised, whilst design of the ammonia storage requirements and power generation needs of the plant have enabled the output of this stage to be designed to minimise the waste output of the plant through stream recycles.

1.12.2   Conclusion

In conclusion, this section of the reactor is vital in providing the long term energy storage. This has meant that scale and reliability has been prioritised in the design, whilst minimising environmental impact and maximising economic efficiency. This satisfies the initial design objectives and meets the needs of respective processes elsewhere in the plant.

1.12.3   Further Design

Whilst this design has addressed all the initial requirements, there are further improvements that could be made to increase efficiency of the process. One of these would be to recycle the hydrogen content within the purge stream, this would not only reduce output wastage but also improve the overall process efficiency.
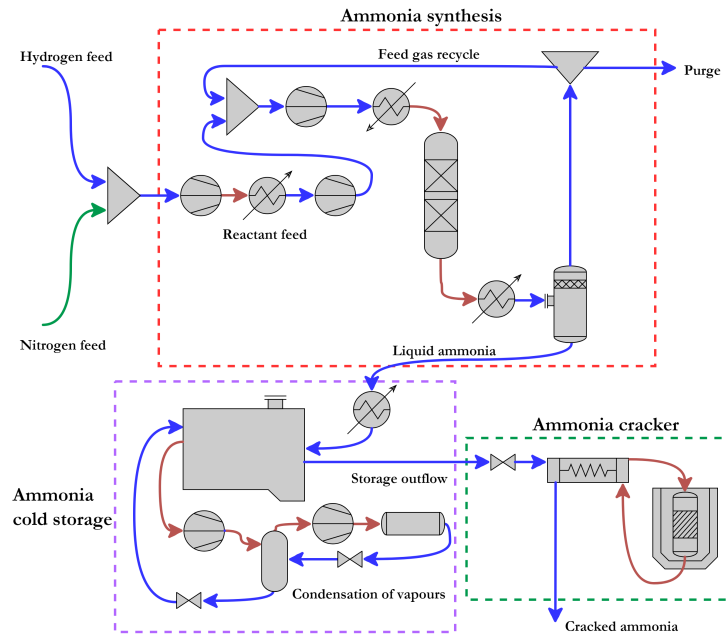
Figure 14: Flowsheet of process

2   Safety and environmental assessment

Ammonia based energy storage systems possess a large number of inherent risks, due to their operating conditions and chemical risks of the materials used. Over the past 50 years one major risk has been plant fires despite a steady decreased over time [27][35]. A number of studies and risk reviews have been conducted on the operation and source of risks and failure within Ammonia synthesis plants [27].

2.1   Chemical risk and hazards

Two most high risk elements of the process are hydrogen and ammonia storage and synthesis. In the case of hydrogen, the main factor is the storage of compressed gas. This is due to the risk of explosion of hydrogen gas under high temperature and pressure. Pressure relief valves can be used to prevent overpressurization and allow the release of gases before fracture of the storage vessel. However, pressure relief can form of explosive hydrogen gas clouds in certain atmospheric conditions and thus adequate monitoring of any valve flow must be made and subsequent ventilation of the outlet gas.

Ammonia has a number of chemical effects; whilst it is not considered a flammable hazardous

product due to its high autoignition temperature (651 °C) and an explosive limit of 16-25% [27], the first of these being its corrosivity to many metals and alloys including copper and zinc, this means that any storage, piping or fittings to come into contact with ammonia should be made only from iron and steel as these do not suffer from ammonia corrosion. Despite its lower density than air evidence suggests that the formation of ammonia gas clouds at ground level is possible in certain environmental conditions [13]. These are largely dependent on wind speed and humidity. The impact of such releases can be varied, and the number of fatalities does not appear to correlate strongly to the amount of ammonia released. A 1400 ton release of ammonia in Lithuania (1989), the largest ever recorded, resulted in a 400km2 affected area and a fatality rate of 7 people, whilst a 38 ton release of ammonia in South Africa (1973) resulted in 18 fatalities, the highest recorded involving ammonia. This was due to the proximity of a urban population, the speed of ammonia release - caused by brittle fracture - and the environmental conditions at the time[27].

Gaseous ammonia can cause severe irritation to the eyes, nose throat and lungs at high enough concentrations whilst contact with liquid ammonia can cause cryogenic burns. The main hazards associated with the levels of toxicity of ammonia and the levels of ammonia associated with each hazard are presented below.

Table 19: Ammonia exposure concentration hazards

Hazard	Concentration (PPM)
Threshold limit value (TLV)	25
Short term exposure limit (STEL)	35
Immediately dangerous to life and health (IDLH)	300
Severe eye and respiratory irritation - Permanent damage	400-700
Convulsive coughing and bronchial spasms	1700
Life threatening	2500
Death from suffocation	5000-10000

Further information on the impact of exposure to ammonia can be found in the Acute Exposure Guideline Levels (AEGS) [25]. In order to minimise the hazards caused by ammonia release, a number of methods are available. The first of these is the positioning of the discharge valve sufficiently high above ground level to allow any high concentrations releases of ammonia to dilute. Furthermore, the installation of a mist extractor prevents liquid droplets of

ammonia being released. This is needed as ammonia is toxic in water ecosystems, a 600 ton spill in Arkansas, USA (1971) resulted in the death of thousands of fish [27].

Despite these measures perhaps the most effective way of minimising the long-term risks is to limit the amount of gas released the plant. This is can be done by recycling streams. In the case of the purge a membrane unit to recover hydrogen. In the ammonia storage tank vented gas is recycled through a refrigeration loop. The ammonia storage tank must be located outside of any plant buildings and at away from any densely populated urban areas. potable water sources and clear of any combustible materials. The site must be easily accessible by road to emergency vehicles and personnel. During any unattended operation constant monitoring of all liquid and vapour levels must take place.

References

[1] L. Aparicio and J. Dumesic. Haber Bosch overall + conv. *Amm. Nitrate Proj.*, 1(9):452, 2008.

[2] A. Araújo and S. Skogestad. Control structure design for the ammonia synthesis process. *Computers and Chemical Engineering*, 32(12):2920–2932, 2008.

[3] R. Bañares-alcántara and M. Fiaschetti. Analysis of Islanded Amm.-based Energy Sto. Sys. (Oct.):1–150, 2014.

[4] J. R. Bartels. A feasibility study of implementing an Ammonia Economy. *Digital Repository @ Iowa State University*, (December):102, 2008.

[5] V. Belapurkar. Boil-Off in Refrigerated Amm. Tanks. pages 1–4, 2016.

[6] J. M. Campbell. Gas-Liquid Separators Sizing Parameter. (December 2014):1–16, 2015.

[7] D. C. Dyson and J. M. Simon. A kinetic expression with diffusion correction for ammonia synthesis on industrial catalyst. *Ind. and Eng. Chem. Fundamentals*, 7(4):605–610, 1968.

[8] S. S. Elnashaie. Response To Comments On Simulation and Optimization of an Industrial Ammonia Reactor. *Ind. and Eng. Chem. Research*, 28(8):1267, 1989.

[9] S. S. E. H. Elnashaie, A. T. Mahfouz, and S. S. Elshishini. Digital simulation of an industrial ammonia reactor. *Chemical Engineering and Processing*, 23(3):165–177, 1988.

[10] S. Ergun and A. A. Orning. Fluid Flow through Randomly Packed Columns and Fluidized Beds. *Industrial & Engineering Chemistry*, 41(6):1179–1184, 1949.

[11] W. Gellett, S. Szymanski, and P. Onsite. High Efficiency Low Cost Production Electrochemical Ammonia Production. *NH3 Fuel Conference, CA*, 2016.

[12] L. J. Gillespie and J. A. Beattie. The thermodynamic treatment of chem. equilibria in systems comp. of real gases. *Jou. of the Amer. Chem. Soc.*, 52(11):4239–4246, 1930.

[13] R. F. Griffiths and G. D. Kaiser. Production of dense gas mixtures from ammonia releases. *Jnl. of Haz. Mat.*, 6(1-2):197–212, 1982.

[14] U. Guacci, F. Traina, G. Buzzi Ferrarla, and R. Barisone. On the Apln. of the Temkin Eqn. in the Eval. of Cat. for the Amm. Synt. *Ind. and Eng. Chem.*, 16(2):166–176, 1977.

[15] V. Hacker, , K. Kordesch, and W. Vielstich. Amm. crackers. *Facilities*, 3:121–127, 2003.

[16] A. M. Howatson, P. G. Lund, and J. D. Todd. Engineering Tables and Data. 1972.

[17] T. B. Jekel, D. T. Reindl, and J. M. Fisher. Gravity Separator Fundamentals and Design. *Ammonia Refrigeration Convention & Exhibition*, (1998):23, 2001.

[18] J. R. Jennings. Catalytic Ammonia Synthesis. Fundamentals and Practice. *Springer Science & Business Media*, page 451, 1991.

[19] A. Jinasena, B. Lie, and B. Glemmestad. Dynamic Model of an Amm. Synt. Reactor Based on Open Inf. *9th EUROSIM Con. on Mod. and Sim. Oulu*, pages 943–948, 2016.

[20] J. Kim, D. Um, and O. Kwon. Hydrogen production from burning and reforming of ammonia in a microreforming system. *Energy Conversion and Management*, 56:184–191, 2012.

[21] V. Kyriakou, I. Garagounis, and E. Vasileiou. Progress in the Electrochemical Synthesis of Ammonia. *Catalysis Today*, 286:2–13, 2017.

[22] H. Liu. Ammonia synthesis catalyst 100 years: Practice, enlightenment and challenge. *Cuihua Xuebao/Chinese Journal of Catalysis*, 35(10):1619–1640, 2014.

[23] H. Z. Liu, X. N. Li, and Z. N. Hu. Development of novel low temperature and low pressure ammonia synthesis catalyst. *Applied Catalysis A: General*, 142(2):209–222, 1996.

[24] Meps. Regional Steel Prices & Indices Country Steel Prices Steel Data. pages 1–2, 2018.

[25] R. Michaels and R. Corp. Emer. Plan.: Crit. Eval. of AEGLs for Amm. 17(2):179–, 1998.

[26] E. R. Morgan. Techno-Economic Feasibility Study of Ammonia Plants Powered by Offshore Wind. *University of Massachusetts - Amherst, PhD Dissertations*, page 432, 2013.

[27] M. Ojha and A. K. Dhiman. Problem , Failure and Safety Analysis of Amm. Plant : a Review. *Int. Review of Chem. En.*, 2(October):631–646, 2010.

[28] M. Penkuhn and G. Tsatsaronis. Comparison of different amm. synt. loop configurations with the aid of advanced exergy analysis. *Energy*, 137:854–864, 2017.

[29] N. Pernicone, F. Ferrero, I. Rossetti, L. Forni, P. Canton, and P. Riello. Wustite as a new precursor of industrial amm. synt. cat. *App. Catalysis A: General*, 251(1):121–129, 2003.

[30] A. Plus. Aspen Plus Ammonia Model. 2008.

[31] J. A. S. Richard Turton, Richard C. Bailie, Wallace B. Whiting. *Analysis, Synthesis and Design of Chemical Processes Third Edition*, volume 53. 2013.

[32] I. Rossetti, N. Pernicone, F. Ferrero, and L. Forni. Kinetic study of ammonia synthesis on a promoted Ru/C catalyst. *Ind. and Eng. Chem. Research*, 45(12):4150–4155, 2006.

[33] Since Gas. Automatic Ammonia Cracker for Hydrogen Generation. pages 4–6, 2018.

[34] M. Souders and G. G. B. Design of Fractionating Columns: I. Entrainment and Capacity. *Ind. and Eng. Chem.*, 26(1):98–103, 1934.

[35] G. P. Williams. Safety perf. in amm. plants: VI. *Proc. Saf. Prog.*, 18(2):78–81, 1999.